Near-Field Magnetophotoluminescence Spectroscopy of Composition Fluctuations in InGaAsN

A. M. Mintairov, T. H. Kosel, and J. L. Merz
EE Department, University of Notre Dame, Notre Dame, Indiana 46556

P. A. Blagnov, A. S. Vlasov, and V. M. Ustinov
Ioffe Physico-Technical Institute, RAS, 194021, St. Petersburg, Russia

R. E. Cook
Argonne National Laboratory, Argonne, Illinois 60439
(Received 4 September 2001; published 10 December 2001)

The localization of excitons on quantum-dot-like compositional fluctuations has been observed in temperature-dependent near-field magnetophotoluminescence spectra of InGaAsN. Localization is driven by the giant bowing parameter of these alloys and manifests itself by the appearance of ultranarrow lines (half-width <1 meV) at temperatures below 70 K. We show how near-field optical scanning microscopy can be used for the estimation of the size, density, and nitrogen excess of individual compositional fluctuations (clusters), thus revealing random versus phase-separation effects in the distribution of nitrogen.

DOI: 10.1103/PhysRevLett.87.277401 PACS numbers: 78.67.Hc, 61.46.+w, 68.37.Uv

$In_xGa_{1-x}As_{1-y}N_y$ ($x = 0-0.08$, $y = 0-0.05$) alloys have recently attracted considerable attention as promising materials for laser diodes in the 1.3–1.5 μm range as well as more efficient solar cells. These applications exploit their unusual electronic property—a "giant bowing" parameter ($b \sim 20$ eV), which arises from the large electronegativity and small size of the nitrogen [1,2]. The giant bowing parameter corresponds to an anomalously strong dependence of the band gap on N content ($dE_g/dy = 15-20$ eV) [3,4], which in turn creates an extremely large energy scale for statistical composition fluctuation in these alloys resulting in strong carrier localization. Indeed, fluctuation of N composition (Δy) of only 0.5% leads to an $\sim$100 meV change in the band-gap energy of InGaAsN. For a spatial scale of the order of 10 nm ($\sim$20 000 atoms) such fluctuation creates a strong confining potential for electrons and holes and will behave as a semiconductor quantum dot (QD), having discrete atomiclike electronic states [5]. An estimation of the probability of occurrence of such QD-like composition fluctuations (clusters) in a random alloy using Stirling's formula gives for $y = 0.02-0.05$ values $10^{-4}-10^{-3}$. This corresponds to a density of the clusters $100-1000$ μm^{-3}, which implies that in an InGaAsN a single cluster can be probed using modern high spatial resolution (<1 μm) optical techniques as widely applied for single QD spectroscopy [6,7]. Thus, due to their unique electronic structure, InGaAsN alloys allow spectroscopic study of individual composition fluctuations, which in turn provide information about random versus spontaneous ordering or phase separation effects in N distribution [8–10]. This is quite important in view of the technological applications of these materials.

In the present paper we used near-field optical scanning spectroscopy to observe emission spectra from N-rich clusters in an $In_xGa_{1-x}As_{1-y}N_y$ ($x = 0.08$, $y = 0.03$) layer, consisting of a short-period $GaAs_{0.966}N_{0.034}/InAs$ superlattice. We observed emission from the single clusters appearing in near-field magnetophotoluminescence spectra of InGaAsN at temperatures below 70 K. The spectra consist of ultranarrow lines with half-width less than 1 meV in an energy range of 1.065–1.095 eV. We measured the average values of the size and N content of the clusters to be 20 nm and 0.035, respectively. The cluster density is estimated to be considerably greater than that expected for a random nitrogen distribution, which indicates their spontaneous formation. The existence of the clusters was confirmed by transmission electron microscope measurements.

The sample used in this study was grown by solid source molecular beam epitaxy on (001) semi-insulating GaAs substrates at $T = 450$ °C. A RF-plasma source was used to generate atomic nitrogen from N_2. A 0.12 μm thick $In_xGa_{1-x}As_{1-y}N_y$ "layer" was grown, consisting of a short period $GaAs_{0.966}N_{0.034}/InAs$ superlattice with individual layer thicknesses 2.82 and 0.25 nm, respectively, giving average In and N compositions $x = 0.08$ and $y = 0.03$. This layer was sandwiched between AlGaAs layers of thickness 60 (bottom) and 14 (top) nm. The structure was capped by a 20 nm GaAs layer and annealed at 730 °C for 10 min. The far-field photoluminescence (PL) spectrum of the InGaAsN layer at 5 K consisted of a single broadband with peak energy 1.088 eV and half-width $\gamma \sim 20$ meV, similar to results reported in the literature [4].

Near-field photoluminescence (NPL) spectra were taken in collection-illumination mode under 514.5 nm excitation by an Ar laser using 20 μW power. We used an uncoated tapered fiber tip that provides spatial resolution of 600 nm (see below). By scanning a 7×7 μm^2 area, this resolution allowed us to rapidly find the same point of the sample for temperature-dependent measurements. Tip-to-surface distance control of the tuning fork was used. The spectra were measured with a single grating spectrometer

with 270 mm focal length, equipped with InGaAs multichannel array detector. The spectral resolution of our system near 1 eV was ~1 meV. The spectra were measured in the temperature range 5–300 K and magnetic field strengths 0–10 T. The magnetic field was parallel to the growth axis.

A cross-sectional specimen was prepared for transmission electron microscopy (TEM) by wedge polishing and Ar ion milling with liquid nitrogen cooling; the final accelerating energy was 500 V. TEM observations were done at 100 kV in a Phillips CM30 microscope.

In Fig. 1 we present NPL spectra taken at different temperatures in the range 10–65 K. We see that at $T = 10$ K the spectra consist of five clearly resolved sharp lines ($\gamma \sim 1$ meV), denoted $C1$–$C5$, superimposed on the broadband ($\gamma \sim 25$ meV), denoted A, centered at 1.084 eV. We can also see several (up to ten) less resolved weak sharp lines. The intensities of the sharp lines dramatically decrease with increasing temperature. The decrease is stronger for higher energies and the lines having energy above 1.08 eV ($C3$–$C5$) disappear in the spectra at ~40 K, while the lines with lower energies ($C1$ and $C2$) disappear at ~70 K. Above 70 K only the A band remains in the spectra. In the inset of Fig. 1 we show temperature dependence of the energy maximum of band A (for $T = 5$–300 K) and lines $C1$ and $C2$ (for $T = 5$–65 K). We can see that for $T > 100$ K the shift of the A band energy follows the behavior typical for band-gap emission of a bulk semiconductor: a decrease of the emission energy with increasing temperature due to thermal expansion, which is well described by the Varshni model [11,12]. For $T \sim 20$–100 K it shows inverted behavior; i.e., the emission energy increases with increasing temperature, which is not described by the Varshni model. This type of behavior occurs in semiconductor alloys due to carrier localization [13] and can be interpreted as carrier capture and switching on of the radiative transitions from deeper lying localized states. The sharp lines $C1$ and $C2$, on the other hand, show normal thermal expansion behavior. We attribute band A to the emission of excitons localized on composition fluctuations having spatial extent $2r$ much greater than the exciton radius (r_{exc}) ~ 10 nm (weak localization regime), and we attribute the C lines to emission of excitons localized on QD-like clusters having $r \leq r_{\mathrm{exc}}$ (strong localization regime). The half-width of the emission spectra reflects in the former case the energy scale of statistical composition fluctuations inside the confinement volume [4], while in the latter case it reflects the δ-function density of states in the quantum dot [5]. The difference between Varshni's model predictions and the energy positions of the emission lines for $T < 150$ (inset of Fig. 1) gives the localization energy for both types of excitons, which is equal to 10–60 meV for $T = 5$ K.

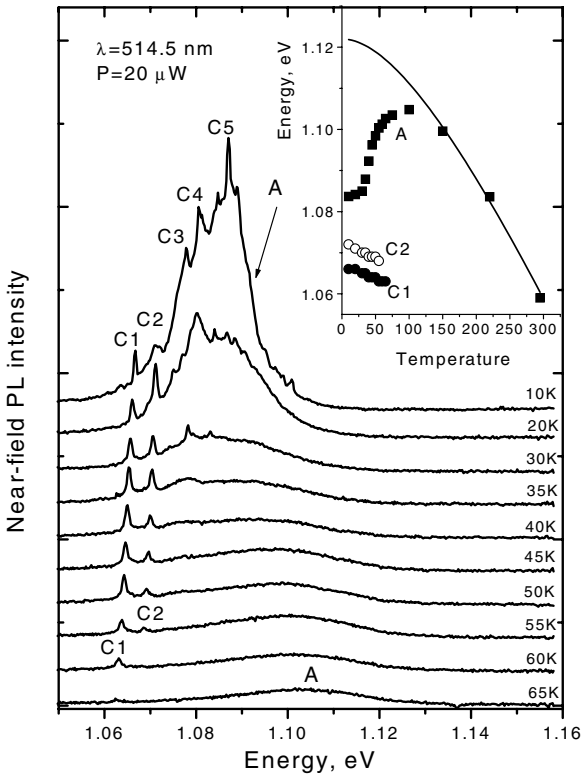

FIG. 1. Near-field PL spectra of $In_xGa_{1-x}As_{1-y}N_y$ ($x = 0.08$, $y = 0.03$) at temperatures 10, 20, 30, 35, ..., 65 K under excitation of 514.5 nm with power $P = 20$ μW. The inset shows the temperature dependence of the maximum of the band A (solid squares) and lines $C1$ (open circles) and $C2$ (solid circles) measured in the spectra and calculated for the A band using Varshni's expression [9] (solid curve).

The evidence that the C-lines emission has QD character (i.e., strong localization regime) was obtained from the diamagnetic shift and Zeeman splitting (see Figs. 2a–2c). The magnetic field behavior for lines $C6$ and $C7$ at 5 K is observed at energies 1.0804 and 1.0828 eV, respectively, as presented in Fig. 2a. The splitting into a doublet (subscript h and l denote high and low energy components) and the high energy shift of the doublet center are clearly seen for these lines for magnetic field strength 4–10 T. The values of the Zeeman splitting of the $C7$ line are 0.6 and 1.7 meV at $B = 4$ and 10 T, respectively (Fig. 2b), which is similar to the values of the splitting of the ground state in QDs [14]. The energy of the center of the $C7$ line doublet shifts quadratically with coefficient $\beta = 9$ μeV/T^2. The diamagnetic coefficient β in QDs can be expressed by [15]

$$\beta = e^2\langle x^2\rangle/8\mu\,, \tag{1}$$

where e is electron charge, $\langle x^2\rangle$ describes the spatial extent of the ground state wave function, and μ is the reduced mass of exciton. Taking the value of the reduced exciton mass in InGaAsN to be $0.139m_0$ [4], we obtain the value of the average radius of the ground state wave function $\sqrt{\langle x^2\rangle} = 7$ nm. It should be noted, however, that expression (1) underestimates the actual radius of a QD by a factor of 2 [15,16], i.e., $r \approx 2\sqrt{\langle x^2\rangle}$. In Fig. 2c we present the values of β and r (where r is the cluster radius)

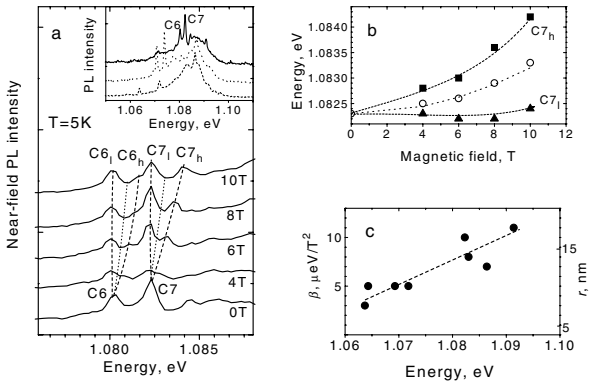

FIG. 2. (a) The 5 K near-field PL spectra of $C6$ and $C7$ line (see inset) at magnetic field strengths $B = 0$, 4, 6, 8, and 10 T. Inset shows near-field spectra taken at three different tip positions separated by ~ 3 μm; (b) dependence of Zeeman splitting (solid triangles and squares correspond to low and high energy components, respectively) and diamagnetic shift (open circles) of $C7$ line as a function of magnetic field strength; (c) the diamagnetic coefficient β (solid circles) versus emission energy of C lines [see inset (a)]. The right vertical axis gives values of the cluster radius calculated from β (see text). The lines are drawn for clarity.

measured for several C lines having different energy (see inset of Fig. 2a). The data show a clear increase of the diamagnetic coefficient with energy, and thus a corresponding increase of the cluster size from 10 to 30 nm with increasing energy. This can be interpreted as a decrease of the size with increasing depth of the composition fluctuation. In contrast to the diamagnetic shift we observed no change of the Zeeman splitting of the C lines with energy. We also find that band A has a diamagnetic coefficient of 45 μeV/T^2, corresponding to $2r \sim 60$ nm, which is consistent with the weak localization regime. Using a calculation of the ground state energy of the particle in the spherical confining region [17] having a radius of 10 nm and localization energy of 40 meV, we calculated the value of the confining potential to be 80 meV [18]. This gives the average value of the composition fluctuation in the cluster to be $\Delta y = 0.5\%$.

For $2r \sim 20$ nm and $\Delta y = 0.5\%$ Stirling's formula gives the probability of cluster formation to be as low as $P_{\text{ran}} \sim 10^{-15}$, which cannot describe the observation of several emission cluster lines in our experiments. Indeed, $P_{\text{ran}} \sim 10^{-15}$ corresponds to an extremely low density of the clusters $\rho_{\text{ran}} = P_{\text{ran}}/V_c \sim 0.2 \times 10^{-9}$ μm^{-3}, where V_c is the cluster volume. Thus for a random alloy, the volume which contains one cluster with probability unity $(1/\rho_{\text{ran}})$ is equal to $\sim 5 \times 10^9$ μm^3. In our experiments an optically excited volume, from which the emission of clusters contributes to the spectra, is determined by the spatial resolution 0.6 μm (see Fig. 3) and layer thickness and is estimated to be ~ 0.03 μm^3. This corresponds to more than 10 orders of magnitude higher density of the clusters and suggests that the formation of the clusters in our sample is spontaneous.

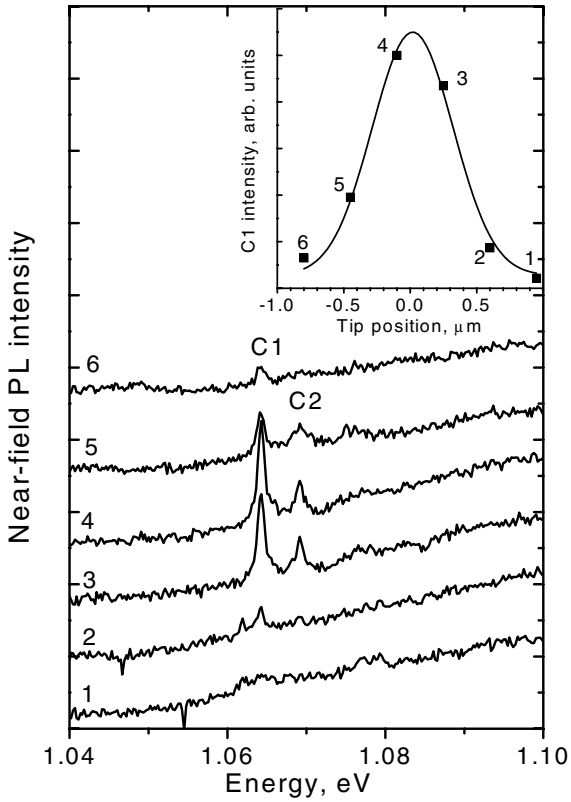

FIG. 3. Near-field PL spectra of InGaAsN ($T = 50$ K) taken at different tip positions along one direction with steps of 0.35 μm. Inset shows the intensity of the $C1$ line versus tip position (solid squares) and the Gaussian contour with half-width 600 nm describing the $C1$ line intensity.

The evidence for cluster formation in our sample was obtained using TEM measurements. In the cross-sectional (004) bright-field image of Fig. 4, we can clearly see the additional contrast superimposed on the superlattice contrast. The contrast corresponding to N-rich clusters appears as a merging of the several superlattice layers and has lateral size 10–30 nm, which is in good agreement with our estimation of the lateral cluster size from near-field magneto-PL spectra.

It should be noted that we also observed sharp emission lines in near-field magnetophotoluminescence spectra of $In_{0.03}Ga_{0.97}As_{0.99}N_{0.01}$, $GaAs_{0.992}N_{0.008}$, and

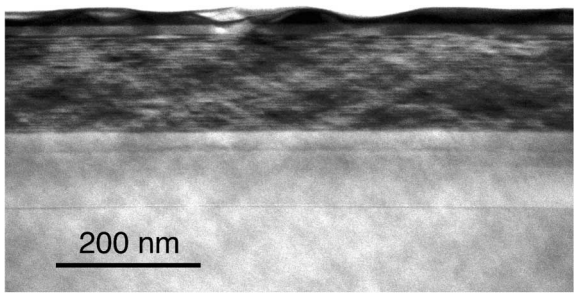

FIG. 4. 004 bright-field TEM image of InGaAsN structure.

$GaAs_{0.97}N_{0.03}$ grown under conditions similar to that of the InGaAsN sample studied in the present paper [19]. The sharp emission lines indicating the presence of quantum-dot-like composition fluctuation was also reported for $GaAs_{0.992}N_{0.008}$ grown by metal-organic chemical vapor deposition [20]. These observations give strong evidence that the formation of the quantum-dot-like compositional fluctuations is an inherent property of InGaAsN alloys.

In conclusion, we have demonstrated that the use of high-spatial-resolution near-field spectroscopy makes it possible to study individual regions of compositional fluctuations in InGaAsN alloys. We have shown that due to the giant bowing parameter and resulting strong carrier localization, the compositional fluctuation in these alloys can behave as quantum dots. A detailed investigation of the near-field magneto-PL yields an estimate of the density, size, and depth of these quantum-dot-like compositional fluctuations, and reveals self-organized effects in the distribution of nitrogen. This is the first of such studies which includes temperature and magnetic-field effects in the wavelength range 1.1–1.2 μm.

The authors acknowledge the W. M. Keck Foundation and the NATO Science for Piece Program (Grant No. SFP-972484) for support of this research. The TEM work at Argonne National Laboratory was supported by the U.S. Department of Energy, Office of Science, under Contract No. W-31-109-Eng-38.

[1] S. Sakai, Y. Ueta, and Y. Terauchi, Jpn. J. Appl. Phys. **32**, 4413 (1993).
[2] S.-H. Wei and A. Zunger, Phys. Rev. Lett. **76**, 664 (1996).
[3] S. Frankoeur *et al.,* Appl. Phys. Lett. **72**, 1857 (1998); J. F. Geiz *et al.,* J. Cryst. Growth **195**, 401 (1998).
[4] E. D. Jones, A. A. Allerman, S. R. Kurz, N. A. Modine, K. K. Bajaj, S. W. Tozer, and X. Wei, Phys. Rev. B **62**, 7144 (2000).
[5] D. Bimberg, M. Grundman, and N. N. Ledentsov, *Quantum Dot Heterostructures* (John Wiley & Sons, Chichester, 1999).
[6] A. Gustafsson, M.-E. Pistol, L. Montelius, and L. Samuelson, J. Appl. Phys. **84**, 1715 (1998).
[7] M. Ohtsu, *Near-Field Nano/Atom Optics and Technology* (Springer-Verlag, Tokyo, 1998).
[8] A. M. Mintairov *et al.,* Phys. Rev. B **56**, 15 836 (1997).
[9] H. A. McCay, R. M. Feenstra, T. Schmidtling, and U. V. Pohl, Appl. Phys. Lett. **78**, 82 (2001).
[10] R. A. Mair *et al.,* Appl. Phys. Lett. **76**, 188 (2000); L. Grenouillet *et al.,* Appl. Phys. Lett. **76**, 2241 (2000); M.-A. Pinault and E. Tournie, Appl. Phys. Lett. **78**, 1562 (2001).
[11] Y. P. Varshni, Physica **34**, 149 (1967).
[12] The parameters of Varshni's expression are $E_g(T) = E_g(0) - \frac{aT^2}{b+T}$, where $E_g(0) = 1.122$ eV, $a = 4 \times 10^{-4}$ K, and $b = 270$ K.
[13] T. Yamamoto *et al.,* J. Appl. Phys. **68**, 5318 (1990); L. Grenouillet *et al.,* Appl. Phys. Lett. **76**, 2241 (2000); M.-A. Pinault and E. Tourne, Appl. Phys. Lett. **78**, 1562 (2001).
[14] S. Brown *et al.,* Phys. Rev. B **54**, R17 339 (1996); W. Heller and U. Bockelman, Phys. Rev. B **55**, R4871 (1997); Y. Toda *et al.,* Phys. Rev. B **58**, R10 147 (1998); M. Bayer *et al.,* Phys. Rev. B **60**, R8481 (1999).
[15] P. D. Wang *et al.,* Phys. Rev. B **53**, 16 458 (1996).
[16] I. E. Itskevich *et al.,* Appl. Phys. Lett. **70**, 505 (1997); L. R. Wilson *et al.,* Phys. Rev. B **57**, R2073 (1998); M. Bayer *et al.,* Phys. Rev. B **57**, 6584 (1998); B. Kowalski *et al.,* Phys. Rev. B **58**, 2026 (1998).
[17] D. B. Tran Thoai, Y. Z. Hu, and S. W. Koch, Phys. Rev. B **42**, 11 261 (1990).
[18] The calculations were done using the values of the effective mass of an electron and hole both inside and outside the sphere as $m_e = 0.24m_0$ and $m_h = 0.35m_0$ and the value of band offsets $\Delta E_c/\Delta E_v$ to be 0.5 and 0.7, respectively. We also neglected the exciton binding energy, which was estimated to be <10 meV, due to the thermal quenching the C-line emission at $T > 70$ K.
[19] A. M. Mintairov *et al.* (to be published).
[20] K. Matsuda *et al.,* Appl. Phys. Lett. **78**, 1508 (2001).